Drawing Equirectangular VR Panoramas with Ruler, Compass, and Protractor

António Bandeira Araújo
Department of Science and Technology,
Universidade Aberta,
Portugal
---
antonio.araujo@uab.pt

ABSTRACT

This work presents a method for drawing Virtual Reality panoramas by ruler and compass operations. VR panoramas are immersive anamorphoses rendered from equirectangular spherical perspective data. This data is usually photographic, but some artists are creating hand-drawn equirectangular perspectives to be visualized in VR. This practice, that lies interestingly at the interface between analog and digital drawing, is hindered by a lack of method, as these drawings are usually done by trial-and-error, with ad-hoc measurements and interpolation of pre-computed grids, a process with considerable artistic limitations. I develop here the analytic tools for plotting all great circles, line images and their vanishing points, and then show how to achieve these constructions through descriptive geometry diagrams that can be executed using only ruler, compass, and protractor. Approximations of line images by circular arcs and sinusoids are shown to have acceptable errors for low values of angular elevation. The symmetries of the perspective are studied and their uses for improving gridding methods are discussed.

KEYWORDS

Visual arts; immersive art; immersive panoramas; VR panoramas; equirectangular perspective; spherical perspective; perspective; drawing; descriptive geometry; digital art; ruler and compass; social networks.

ARTICLE INFO

Received: 02 January 2018
Accepted: 21 February 2018
Published: 03 April 2018

https://dx.doi.org/10.7559/citarj.v10i1.471

1 | INTRODUCTION

1.1 PREVIOUS WORK

This work intends to settle equirectangular spherical perspective as a proper perspective, by providing clear and complete rules to solve all lines and vanishing points, and a method for drawing them with simple tools. It aims to bridge the gap between traditional and digital drawing, in the creation of immersive VR panoramas. This is a revision and expansion of previous results I presented in a recent conference paper (Araújo, 2017).

1.2 MOTIVATION

Artists are subverting Virtual Reality panoramas. VR panoramas have been integrated into social networking platforms mostly to accommodate photographic pieces generated by 360-degree cameras. Such cameras create equirectangular spherical perspective pictures and the VR software provides an immersive experience, by monitoring the viewpoint of the user's mobile phone or headset and rendering at each instant a plane perspective of a certain field of view from within the total picture. Facebook, Google, and Flickr all provide simple ways for the user to upload these pictures and share them as VR, and specialized services keep popping up, such as Kuula, offering new variations and features for their display. But as this integration grew, some artists started tentatively hand drawing – rather than shooting - they own panoramas. Once uploaded, these drawings will "look right" as VR panoramas if they follow the rules of equirectangular perspective. There's an interesting collection of such drawings appearing at Flickr's artistic panorama group (Art Panorama Group, 2017). See also the whimsical examples by David Anderson (Anderson,

n.d.) and the virtuoso on-location drawing by Gérard Michel (Michel, 2007; 2017).

This interest in drawing VR panoramas is part of a trend. Illustrators and urban sketchers (the present author hails from both tribes) seem of late rather keen on curvilinear perspectives and anamorphoses. Such waves of enthusiasm arise whenever anamorphosis finds a new technological expression. The current VR experience rehashes that of once popular 19th century panoramas, for the display of which large rotundas were built (Huhtamo, 2013), or the immersive spectacle of illusionary church ceilings. These large scale immersive anamorphoses were drawn out in plan and elevation as if to build real architecture (and sometimes in replacement of such, as in the case of Andrea Pozzo's famous dome at Sant'Ignazzio's (Kemp, 1990), and then painted as a 2D simulacrum of the imagined object. VR panorama drawings work much the same way. Here too the artist starts with a flat perspective drawing and aims at an immersive experience. The obvious difference is in the technology. A further, crucial difference, concerns us here: When Andrea Pozzo did his illusionary work in the late 1600s, he was firmly grounded in the knowledge of linear perspective, as his treatise attests (Pozzo, 1700); crudely put, he knew what he was doing. By contrast, our VR panorama makers have no handy equirectangular perspective manual they can rely upon. What is available addresses computer rendering, not human drawing. Artists do without it in their usual fashion, being notorious hackers of ad-hoc perspective, classical or otherwise, who will - quite rightly! - cheat and fake it if they must, by sheer trial-and-error, by drawing over pre-computed grids or on top of photographs.

But it is lamentable to have to settle for such crude methods. It can be argued that technology tends to generate ignorance of the very processes it streamlines (Stiegler, 2010), and this is true in particular of the naive use of digital tools in art (Rodriguez, 2016). That you can click a menu and get a perspective grid does not enhance your knowledge of perspective. It hinders it, by making it unnecessary. That knowledge gets expressed in the machine's primitive operations rather than the human's (brute force plots rather than judicious ruler and compass operations) and then black-boxed out of view through abstraction and encapsulation, which itself limits one's modes of thought and expression (Papert & Turkle, 1991); instead of learning perspective you learn to turn knobs on a black box whose interface delimits the scope of your imagination. There is a knowledge of space and form that you only get from drawing with your hands and computing with your brain. That you can get a perspective at the click of a button only makes it more urgent that you know how to get one through your mind and hands.

I argued, in a recent paper (Araújo, 2017b), for a "deliberate rudimentarization" or "cardboarding" in teaching the concepts behind digital tools - exposing the conceptual gears of digital black boxes by reducing them to their most basic physical expression. The aim is to translate between the human and the machine-executable, creating digital-analog feedback loops that enhance the understanding of both realms, and create spots for artistic intervention upon the tools themselves. The connection between anamorphoses, descriptive geometry (DG) and Mixed Reality (MR) is one such example of feedback loop. Through analog DG techniques (Araújo, 2017a), the student can build illusory objects that can be shared through digital photography (the camera being the perfect cycloptic eye of perspective), in a way that both motivates the learning of DG techniques and illuminates the operations behind MR tools. VR panoramas can expand on this approach since they enable the sharing in social networks not only of the static photograph of the resulting anamorphosis, but the actual immersive experience of the imagined object's visual presence. Note that curvilinear perspectives are intimately related to anamorphoses. A perspective can be seen as an entailment of two maps - a conical anamorphosis followed by a flattening (Araújo, 2015). Usually the anamorphosis remains merely conceptual - although some artists, notably Dick Termes (Termes, n.a.) have explored it explicitly - as the artist works directly on the perspective due to the convenience of drawing on a plane. The VR display reverses the entailment, allowing for an analog spherical perspective, drawn by hand, to acquire its anamorphic (mimetic) character. As a didactic tool this allows the student to check the correctness of his perspective construction in the most direct manner. A curvilinear perspective drawing can be hard to interpret, but an anamorphosis is judged by eye: a line, planned out in spherical perspective, either looks straight in VR or it doesn't - allowing for

Figure 1 | Equirectangular panorama of a cubical room seen from its center (left), compared with azimuthal equidistant perspective of the same (right). Drawings by the author. The VR panorama rendering is available at the author's website (Araújo, 2017c).

an experiential confirmation of the successful perspective drawing. This specific type of visualization will in turn feed back into the drawing process, nor merely as a verification tool but as a motivator of specific aesthetics (the VR display is a reading mode and there is no such thing as a passive reading mode) and therefore of the need to solve geometric problems that derive from these aesthetic goals.

But if the VR panorama is to have such didactic applications, a clear method is required to plot the perspectives by hand, not only within precomputed grids (which are just another black box), but for all general line projections. That is, one must solve the perspective. This is what I propose here, in two parts: First I develop the analytic and computational tools for the systematic plotting of great circles, straight line images and their vanishing points. Next, I provide diagrammatic methods to achieve these constructions without a computer, so as to draw general equirectangular projections, from observation or orthographic plans, using only ruler, compass, and protractor.

2 | SOLVING EQUIRECTANGULAR PERSPECTIVE

A spherical perspective can be defined as a conical anamorphosis onto a sphere followed by a flattening of the sphere onto a plane (Araújo, 2015). The anamorphosis is just the central projection map $P \mapsto \overrightarrow{OP}/|OP|$ where O is the center of the sphere, representing the viewpoint. It is the same for any spherical perspective, and turns spatial lines into meridians with exactly two antipodal vanishing points. Hence it is the choice of the flattening map that distinguishes between spherical perspectives. These flattenings are usually cartographic maps, chosen for some useful property. For instance, the most well-known example of a spherical perspective, and the first to be solved by elementary means (Barre & Flocon, 1964), was defined by choosing the azimuthal equidistant map projection for its flattening. In the anterior hemisphere, this flattening shows low deformations and turns meridians into (approximate) circular arcs (Barre, Flocon, & Bouligand, 1964); in the posterior hemisphere, it turns meridians into curves that are constructible from circular arcs by simple ruler and compass operations (Araújo, 2015). The simplicity of these line projections makes it a strong choice for a hand-drawn perspective. In contrast, equirectangular line projections (meridians) are clearly not as simple as arcs of circle, as can be seen in a comparison of the two projections in Figure 1. Equirectangular perspective has, however, some important advantages: it is the standard input for VR panorama rendering engines, so it skips a conversion step that tends to generate troublesome artefacts; its coordinates correspond to the natural angles that one measures in surveying; it renders onto a rectangle rather than a disc, which accords well both with image files and with the usual shape of drawing pads, sketchbooks and picture frames; and, as we shall see, it has many of the useful features of cylindrical perspective with the advantage of covering the whole field of view. For all these reasons, it would be useful to solve this perspective. To *solve* a perspective means to give a classification of all lines and of their vanishing points, and a method to plot them in practice. It also implies a specification of means. Equirectangular perspective is trivially plotted point-by-point by a computer, but we want it to be solvable with simple

tools. The usual candidates are ruler and compass. To tackle equirectangular perspective we need to add to these a protractor.

2.1 THE EQUIRECTANGULAR MAP PROJECTION AND ITS PERSPECTIVE

Let us define the equirectangular perspective image of a point P. As discussed above, it is a two-step process. P is first projected radially onto the sphere surface. Then that image point P' is flattened onto the plane by the equirectangular map projection. This cartographic projection maps a point of the sphere onto its longitude (λ) and latitude (φ) coordinate pair, (λ, φ) (Snyder, 1987). It maps the sphere onto the 2×1 rectangle $]-180°, 180°[\times]-90°, 90°[$ and turns parallels and (north-south) meridians into horizontal and vertical straight lines, respectively (Figure 2). Note that we will mostly measure angles in degrees rather than radians (asking the reader to mind the trigonometric conversions assumed) since degrees are so convenient for drawing (an A3 sheet will nicely fit a 360x180[mm] drawing rectangle, with longitudes in the interval [-180mm,180mm] and latitudes in [-90mm,90mm]. We choose a right-handed orthonormal referential $(\overrightarrow{u_x}, \overrightarrow{u_y}, \overrightarrow{u_z})$ at the center of the sphere O, such that (x, y) is the equatorial plane, $\overrightarrow{u_z}$ points at the north pole, and $O + \overrightarrow{u_x}$ has zero longitude. Then by simple trigonometry applied to Figure 2, we see that $\varphi = \arcsin\left(z/\sqrt{x^2+y^2+z^2}\right)$. As for λ, it equals $\arctan(y/x)$ when $x > 0$. For $x \leq 0$ we must add or subtract 180º to this, for $y \geq 0$ or $y < 0$, respectively, and settle the $x = 0$ case by continuity. The case $x = y = 0$ is undefined. This is neatly summed up by the function $atan2(y, x) = Arg(x + iy)$, the so-called four-quadrant inverse tangent, that verifies $atan2(\cos(\theta), \sin(\theta)) = \theta$ for $\theta \in]-180°, 180°]$. Hence the equirectangular perspective is given by the $\mathbb{R}^3 \to \mathbb{R}^2$map

$$(\lambda, \varphi) = \left(\text{atan2}(y, x), \arcsin\left(\frac{z}{\sqrt{x^2+y^2+z^2}}\right)\right).$$

This verifies the technical conditions for a curvilinear perspective specified by (Araújo, 2015), namely: the flattening is a homeomorphism in a dense open subset of the sphere, and its inverse can be extended to a continuous map between compact sets. In fact, the flattening is one-to-one outside of the north-south meridian m that goes through $(-1,0,0)$, and its inverse can be extended by

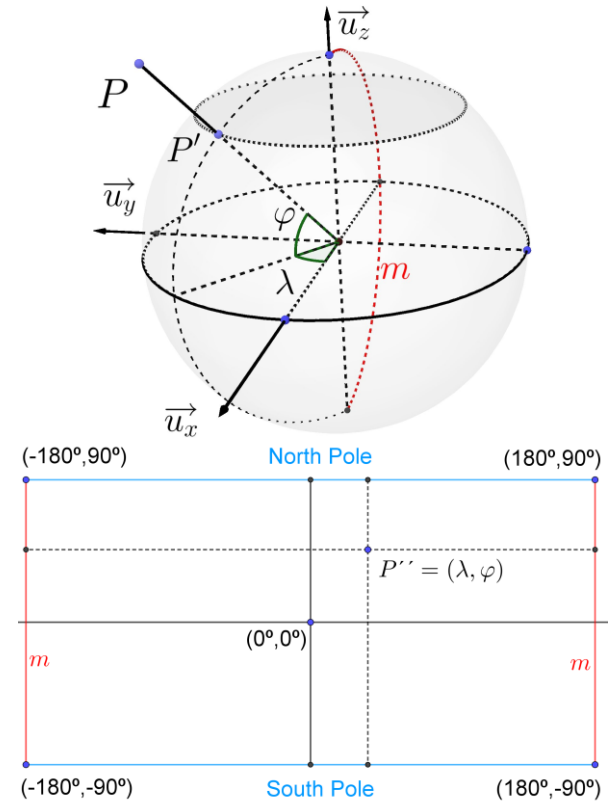

Figure 2 | Equirectangular perspective and flattening. P maps to P' on the sphere by central projection and onto P'' on the rectangle of the perspective drawing.

continuity to map the closed 2×1 rectangle to the whole sphere, by the continuous map

$$(\lambda, \varphi) \mapsto (\cos(\varphi)\cos(\lambda), \cos(\varphi)\sin(\lambda), \sin(\varphi))$$

that sends the top and bottom edges of the rectangle to the north and south poles respectively, and sends both vertical edges to the meridian m (Figure 2).

2.2 ON LINES AND VANISHING POINTS

Solving a perspective requires a classification of spatial lines and their vanishing points. How you classify spatial lines depends on what you can measure. An architect, drawing from plan and elevation, can measure lengths. An astronomer measures angles from a fixed point. The draughtsman finds himself in the latter's position when drawing from life. I will now define what for such a draughtsman may be a natural set of variables to classify spatial lines.

Given a spatial line l, it is often possible to identify the direction of the vertical plane *H* where it lies. Suppose the viewer rotates (to a given longitude λ_0) to face this plane. Then l will extend 90 degrees to his left and right, going to its vanishing points. The

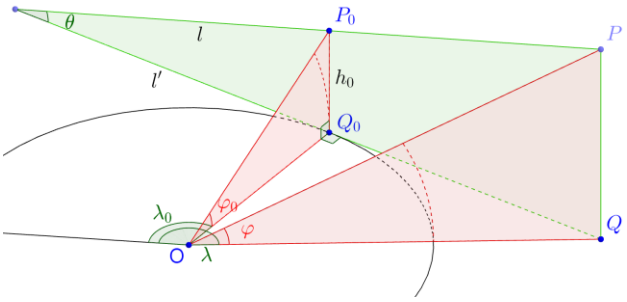

Figure 3 | Angular coordinates of a generic spatial line.

viewer can measure the incline of l (the angle θ that l makes with the horizontal through *H*) by tilting a pencil on a plane parallel to *H* while visually superimposing it on l (the angle is preserved by triangle similarity). Finally, he can measure the angular elevation φ_0 at which l passes in front of him. We thus get coordinates $(\lambda_0, \varphi_0, \theta)$ that fully specify line l.

Now we'd like to know how to plot such a line. If l is contained on a vertical plane through $O (O \notin l)$, then it's trivial: l projects onto a vertical line (if l is vertical) or onto two antipodal vertical line segments differing by 180º in longitude.

Let us consider then the non-trivial case: Let l be a spatial line such that $O \notin l$ and l is not on a vertical plane through O. We start by defining our three line parameters more carefully: Let l' be the orthogonal projection of l onto the equatorial plane. There is a point Q_0 such that OQ_0 and l' define a right angle (Figure 3). Let λ_0 be the longitude of Q_0. Let P_0 be the point of l lying on the vertical plane through OQ_0. Let φ_0 be the latitude of P_0. Let θ to be the incline of l, i.e., the angle between l and l' on the vertical plane through l. We wish to plot a generic point P on the line l of coordinates $(\lambda_0, \varphi_0, \theta)$. We will determine an expression $\varphi(\lambda) = f(\lambda|\lambda_0, \varphi_0, \theta)$ for the latitude φ of P in terms of its longitude λ. Let Q be the orthogonal projection of P onto the equatorial plane. Let $\Delta x = |Q_0Q|$, $d_0 = |OQ_0|$, $h_0 = |Q_0P_0|$. Then

$$\varphi(P) = \arctan\left(\frac{|PQ|}{|QO|}\right) = \arctan\left(\frac{h_0 + \tan(\theta)\Delta x}{\sqrt{d_0^2 + \Delta x^2}}\right)$$

$$= \arctan\left(\frac{h_0/d_0 + \tan(\theta)\Delta x/d_0}{\sqrt{1 + (\Delta x/d_0)^2}}\right)$$

$$= \arctan\left(\frac{\tan(\varphi_0) + \tan(\theta)\tan(\lambda - \lambda_0)}{\sqrt{1 + \tan^2(\lambda - \lambda_0)}}\right)$$

$$= \arctan(\cos(\lambda - \lambda_0)(\tan(\varphi_0) + \tan(\theta)\tan(\lambda - \lambda_0)))$$

$$= \arctan(\tan(\varphi_0)\cos(\lambda - \lambda_0) + \tan(\theta)\sin(\lambda - \lambda_0))$$

Hence the line of coordinates $(\lambda_0, \varphi_0, \theta)$ has parametrization $\lambda \mapsto \varphi(\lambda) = f(\lambda|\lambda_0, \varphi_0, \theta)$

$$= \arctan(\tan(\varphi_0)\cos(\lambda - \lambda_0) + \tan(\theta)\sin(\lambda - \lambda_0)) \quad (1)$$

where $\lambda \in [\lambda_0 - \pi/2, \lambda_0 + \pi/2\,]$.

Let us use this to plot some lines and get a feel for their appearance. First, we note that spatial rotational symmetries around the z axis become translational symmetries for λ. We see that $f(\lambda|\lambda_0, \varphi_0, \theta) = f(\lambda - \lambda'|\lambda_0 - \lambda', \varphi_0, \theta)$ for any λ'; in particular, $f(\lambda|\lambda_0, \varphi_0, \theta) = f(\lambda - \lambda_0|0, \varphi_0, \theta)$, so we can draw any line as if it lies on the $\lambda_0 = 0$ vertical plane, and then shift it sideways to its correct position on the perspective plane. This reduces the drawing problem to the $\lambda_0 = 0$ case.

Let's begin by drawing horizontals. Then $\theta = 0$, and our parametrization simplifies to $f(\lambda|\lambda_0, \varphi_0, 0) = \arctan(\tan(\varphi_0)\cos(\lambda - \lambda_0))$. The plot looks sinusoidal up to around the 45º mark, and then grows squarish as φ_0 approaches 90º degrees (Figure 4 (top)). Notice the mirror symmetry around $\lambda = \lambda_0$, and the translational symmetry that allows us to plot a full grid (Figure 4 (top)) of horizontals (and verticals) by just calculating the central family and then sliding three copies to the side by 90º increments. All in all, horizontals don't look too complicated. General lines are another matter: In (Figure 4 (bottom)) I plotted three families of parallel

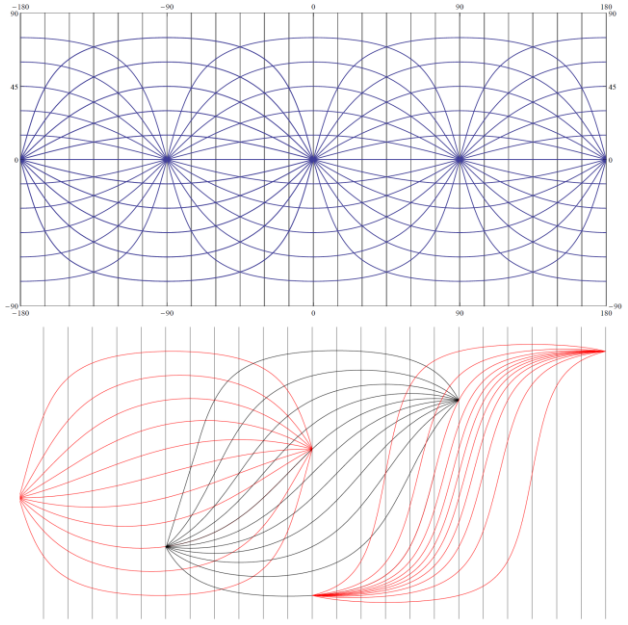

Figure 4 | Top: Grid of horizontal and vertical lines at 15º intervals. Bottom: Sets of parallels with incline equal to 15º, 45º, and 75º. When $\varphi_0 = 0$, the incline of the image at the equator equals the true incline of the spatial line on its vertical plane.

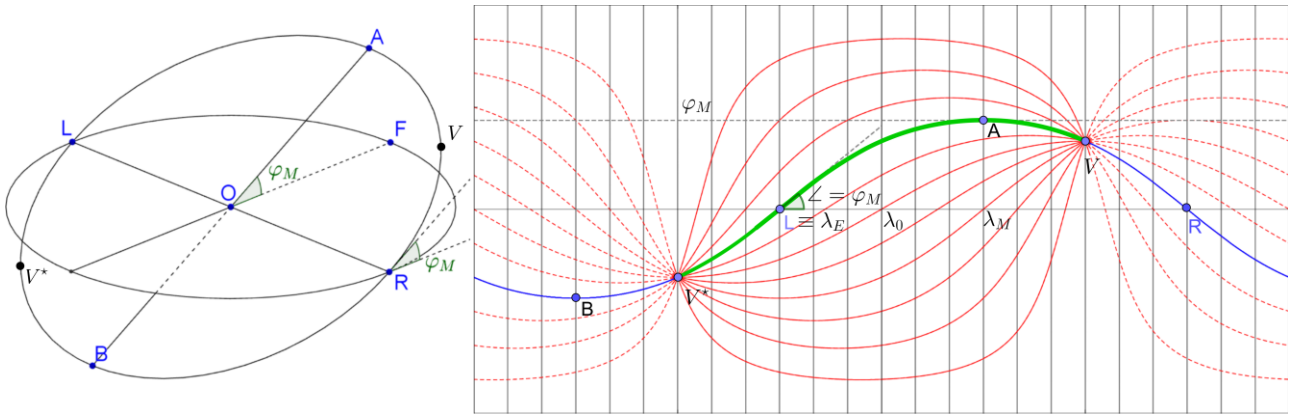

Figure 5 | Left: the plane of a great circle (λ_M, φ_M) = LARB. Right: the image of a set of parallels (red) and their great circles (dashed), with (λ_M, φ_M) in blue and green. Line $V^\star AV$ (green) has $\theta \neq 0$ but shares the plot of horizontal line $LAR = (\lambda_M, \varphi_M, 0)$, both being meridians of the same circle. The incline of the projected great circle equals φ_M at λ_E.

lines. From left to right we have θ =15º, 45º and 75º, with $\lambda_0 = -90º$, 0º, 90º respectively, and lines in each family separated by intervals of 15 degrees of latitude. We see that as θ grows the lines become S-shaped, and then progressively sigmoidal, with the maximum of the curve being reached closer and closer to the vanishing point. Individual lines are no longer mirror symmetric across the $\lambda = \lambda_0$ axis, only the $\varphi_0 = 0$ line of each family retaining central symmetry. These curves seem rather daunting to the unaided analog artist!

Fortunately, there is a way to reduce all lines to the $\theta = 0$ case. In any spherical perspective is it always smart to draw a line by first drawing its great circle and then finding the line inside it. A line projected on a sphere is always a meridian (half of a great circle), and a great circle projects either as a vertical or as a union of two horizontals (Figure 5) oriented at some angle λ_M. We will find that angle, those horizontals, and our line within them, as a subset delimited by its two vanishing points. Start by recalling some spherical geometry: The antipodal point of a point P is the point $P^\star$ diametrically opposite to it on the sphere. If $P = (\lambda, \varphi)$ then $P^\star = (\lambda - sgn(\lambda)\pi, -\varphi)$ where $sgn(x) = x/|x|$. A great circle is the intersection of the sphere with a plane through its center. A spatial line defines such a plane; Hence a spatial line defines a single great circle and projects as a meridian, the great circle being the union of two meridians whose points are antipodal to each other. The vanishing points of the line, that delimit it inside its great circle, are obtained (in any central perspective) by translating the line to O and intersecting with the sphere. Hence a line $(\lambda_0, \varphi_0, \theta)$ has vanishing points at $v_1 = (\lambda_0 - sgn(\lambda_0)\pi, \theta)$ and at its antipode $v_1^\star$. We now note that our parametrization of a line (hence, of a meridian) can already be used to plot the whole great circle that contains it, simply by extending its domain while preserving its functional form. In fact, let C be the great circle of l. Then the perspective image of C is the union of the image of l with the set of the images of the antipodal points of l. But from eq. 1 we see that $\varphi(\lambda - sgn(\lambda)\pi|\lambda_0, \varphi_0, \theta) = -\varphi(\lambda|\lambda_0, \varphi_0, \theta)$, since the sin and cos reverse sign and arctan is odd, so the function $\lambda \mapsto f(\lambda|\lambda_0, \varphi_0, \theta)$ already parametrizes the whole great circle of l if we extend its domain to $[\lambda_0 - \pi, \lambda_0 + \pi]$. Further, we can rewrite the parametrization to get a single cosine in the arctan argument. Just set $C\cos(\lambda - \lambda_M) = \tan(\varphi_0)\cos(\lambda - \lambda_0) + \tan(\theta)\sin(\lambda - \lambda_0)$ for unknown λ_M , C. Setting $\lambda = \lambda_0$we get $C\cos(\lambda_0 - \lambda_M) = \tan(\varphi_0)$, and setting $\lambda = \lambda_0 + \pi/2$ we get $C\sin(\lambda_0 - \lambda_M) = -\tan(\theta)$, whence $C^2 = \tan^2(\varphi_0) + \tan^2(\theta)$ and $\lambda_M = \lambda_0 + \arctan(\tan(\theta)/\tan(\varphi_0))$. Then the parametrization of the great circle containing line $(\lambda_0, \varphi_0, \theta)$ takes the form

$$g(\lambda|\lambda_M, \varphi_M) = \arctan(\tan(\varphi_M)\cos(\lambda - \lambda_M)) \qquad (2)$$

where $\lambda \in [-\pi, \pi]$, and

$$\lambda_M = \lambda_0 + \arctan(\tan(\theta)/\tan(\varphi_0)),$$
$$\varphi_M = \arctan(\sqrt{\tan(\varphi_0) + \tan(\theta)}).$$

We see that a great circle is therefore described by the pair of parameters (λ_M, φ_M) . We have $f(\lambda|\lambda_0, \varphi_0, \theta) = g(\lambda|\lambda_M, \varphi_M)$ when $\lambda \in [\lambda_0 - \pi/2, \lambda_0 + \pi/2]$, so that both parametrize the same line in a given window of width π. But notice that (2) has the functional form the plot of a horizontal! It is the plot of the horizontal $(\lambda_M, \varphi_M, 0)$ when λ is in the interval $[\lambda_M - \pi, \lambda_M + \pi]$ and of its antipode $(\lambda_M \pm \pi, -\varphi_M, 0)$ outside of that interval. That means we can draw any line by drawing horizontals and clipping them at

the line's vanishing points! Figure 5 clarifies the geometric meaning of the pair λ_M, φ_M. On Figure 5 (left) we see a great circle $C = ARBL$ and on Figure 5 (right) its perspective image (blue and green line). The plane of the great circle intersects the equatorial plane at a line LR and makes an angle φ_M with it. This angle equals the maximum latitude reached by C, at point A with longitude λ_M. Note that φ_M also equals the incline of the tangent at the latitude λ_E where the circle crosses the equator. Since tangents are preserved at the equator, the plot has incline φ_M at longitude λ_E. This and the zero incline at λ_M gives the draughtsman useful control points for the tangents. Note that a line with $\lambda_0 = \lambda_E$ has $\theta = \varphi_M$; a line with $\theta = 0$ has incline $\varphi_0 = \varphi_M$ at its vanishing points; and a line with $\varphi_0 = 0$ has latitude $\theta = \varphi_M$ at its vanishing points. λ_M and φ_M define the circle uniquely, but there are many meridians (lines) in it; we write $l \equiv l'$ when lines l, l' share the same great circle. To specify a line, we set either λ_0 or a vanishing point V. This defines a 180º clipping window (the interval $[\lambda_0 - \pi, \lambda_0 + \pi]$) where line $V^\star AV$ (in green on Figure 5, right) lies on the plot of the complete great circle (in blue). Note that on the plot, latitude rises from $V^\star$, goes to zero at λ_E, passes through φ_0 and reaches its maximum over λ_M, then declines towards V. It has incline φ_M at longitude λ_E, as discussed. We see that the asymmetrical plot of the line is just a section of the more symmetrical plot of the great circle in blue, and this is just the union of two mirrored horizontals. In fact, $(\lambda_M - \pi/2, 0, \varphi_M) \equiv (\lambda_M, \varphi_M, 0)$. We illustrate this for a family of parallels. In Figure 5 (right) we draw in filled red. They have vanishing points at $(\pm 90°, \pm 30°)$, so $\lambda_0 = 0$, and their range is $[-90°, 90°]$. They all have incline $\theta = 30°$ and differ by 15º increments in λ_0. By plotting their full circles (dashed red) we see how they are nothing more than a plot of horizontals as in the grid of Figure 4 and the asymmetry is an artefact of their sampling by the clipping window. All we need to draw are horizontals $(\theta = 0)$ lines and their lateral translations. For instance, for our green line, which is $(0, 30°, 30°)$, we obtain from the definitions in eq. 2 that $\lambda_M = 45°$ and $\varphi_M = \arctan(\sqrt{(2/3)}) \approx 39°$, so we plot the horizontals $(45°, 39°, 0)$ and $(135°, -39°, 0)$ which together make up the circle $(45°, 39°)$, and then clip it at $\lambda = \pm 90°$. Of course we'd rather not use the expressions of eq. 2 to obtain (λ_M, φ_M). We don't wish to draw with calculator in hand. But we can measure them directly from observation. On the domain of a line you always have one of the extremes and one points where it hits the equator. If λ_E is easier to spot, find it and you know λ_M is 90º away; then measure the angular height at λ_M to get φ_M. Or measure the incline at λ_E, and recall it must equal φ_M. For instance, for our blue line, the incline at $\lambda_E = 45°$ is $\varphi_M \approx 39°$.

2.3 PLOTTING WITH RULER, COMPASS AND PROTRACTOR

We have reduced all line plots to those of type $(0, \varphi_M, 0)$, modulo translation and choice of vanishing points. It remains to show how to plot these lines by elementary means, using ruler, compass, and protractor, rather than computers or calculators. We will do it with some simple descriptive geometry diagrams.

We work on the setup of construction of Figure 6 (left), which is nothing more than an orthographic view of the general scheme in Figure 3 for the case $\theta = 0$. The following construction obtains φ for a given λ. It can be seen as a graphical algorithm that takes λ as input and outputs $\varphi(\lambda) = f(\lambda|0, \varphi_0, 0)$, the protractor serving as the input-output interface and the ruler and compass providing the operations of the (analog) computer:

1. Draw a vertical segment $\overline{OQ_0}$ of arbitrary length. Draw perpendiculars to $\overline{OQ_0}$ through O and Q_0. Let these be l_O and l' respectively.
2. With a protractor, find H on l' such that $\angle Q_0 O H = \varphi_0$. With center on Q_0 draw a circle through H, to find P_0 on QQ_0. Draw a horizontal l through P_0.

Steps 1 and 2 set up our machine for the line $(0, \varphi_0, 0)$. Now we are ready to use it (Figure 6 (right)):

3. Input λ: With a protractor, find Q_λ on l' such that $Q_\lambda O Q_0 = \lambda$.
4. Operation: With center at Q_λ, draw a circle through O to find O_λ on l'. Then $|O_\lambda Q_\lambda| = |OQ_\lambda|$. Draw a vertical through Q_λ to find P_λ on l.
5. Output: Read $\varphi(\lambda) = \angle P_\lambda O_\lambda Q_\lambda$ with a protractor.

In Figure 7 (top) we used this construction to draw one quarter of the great circle $(0, 80°)$, or half of the line $(0, 80°, 0)$ (Figure 7 (bottom)). The rest of the great circle can be obtained from this section by mirror and central symmetry. Six points were found

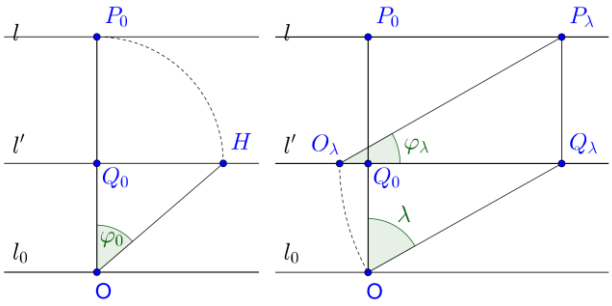

Figure 6 | Left: Setup of orthographic view for calculating $\varphi(\lambda)$ of a $(0, \varphi_\lambda, 0)$ line. Right: Finding the latitude $\varphi(\lambda)$ for a given longitude λ.

(with errors in the order of one degree) and the rest were interpolated by eyeballing constant curvature segments (arcs of circle) between each consecutive set of three points. Besides these six points we know both the longitudes and the tangent inclines at λ_M and λ_E (the incline at λ_E equals $\varphi_M = 80°$ and is null at λ_M). These control points for the tangents help us direct the drawing of the curve. We can see that even at this high value of latitude, as few as three judiciously chosen points would still provide a serviceable approximation to the curve.

Application to the $\theta \neq 0$ case: The construction above could be trivially applied to lines with $\theta \neq 0$ with a simple modification to step 2: draw line l on step 2 with incline θ. The rest of the procedure is identical. But doing this makes for an unwieldy diagram. It is easier to use this diagram to find (λ_M, φ_M), then reduce the problem to the corresponding one of type $\theta = 0$ through longitudinal translation and apply the procedure described above. To obtain (λ_M, φ_M) from $(\lambda_0, \varphi_0, \theta)$ (as an alternative to direct measurement or calculation) do as follows: on step 2, draw l with incline θ. Find the intersection of l with l'. Let this intersection be QE. Then measure $Q_0 O Q_E$ with a protractor to obtain λ_E.

Having learned to find all vanishing points and plot all great circles, we can now build complex scenes as the example of Figure 10, with ramps that climb up or down at arbitrary angles.

A note is in order at this point. One might reasonably doubt the worth of using descriptive geometric constructions to obtain what a pocket calculator can do in seconds. The point is that with this last step, by avoiding all explicit numerical calculations, we have placed equirectangular perspective into the very small set of perspectives that can be fully constructed within that geometric tradition that

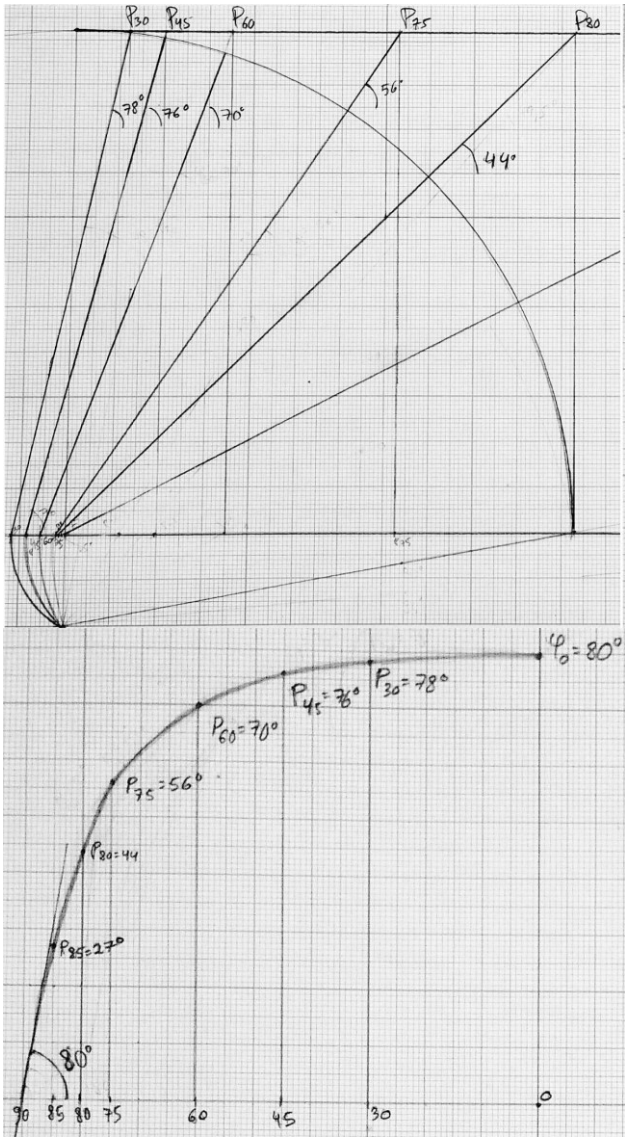

Figure 7 | Calculation with ruler, compass and protractor (top), of one half of the line (0, 80º, 0) (bottom).

connects Euclid, Alberti, and Monge. It is also perhaps unexpected, hence worth noting, the simplicity of the operations required.

2.4 APPROXIMATIONS

We note that, for small φ_0, equirectangular perspective looks very similar to cylindrical perspective. It is to be expected that sinusoids will approximate horizontals reasonably well. Circular arc approximations also turn out to be useful. Both these curves are easily plotted by ruler and compass (or freehand). In both cases we approximate the equirectangular plot of the horizontal line $(0, \varphi_o, 0)$ by the single sinusoid/arc-of-circle that coincides with it at the apex $(0, \varphi_o)$ and at the vanishing points $(\pm 90°, 0)$. These approximations are plotted in Figure 8 (top). We see that for $\varphi < 35°$, the sinusoid is a good approximation (max. error $\approx 1°$), and just

Table 1 | Errors of sinusoidal/circular approximations.

φ_0	15º	30º	35º	40º	45º	50º	60º
Maximum errors in absolute value:							
sin	0,1º	1.1º	1.8º	2.8º	4º	6º	11º
circ	0.8º	1.5º	1.7º	1.8º	1.8º	1.9º	1.9º

as it collapses (see Table 1) the circle becomes a better approximation and remains so until about $\varphi_0 = 60^\circ$ (max. error $\approx 2^\circ$). In Figure 8 (bottom) we can see a plot of the approximation errors. The sinusoids have always positive error with a single maximum on each side, always located close to the 60º latitude. The circles have a more complex behavior, starting with single-minimum negative errors and then developing two extrema, one positive and one negative, whose locations travel towards the 90º mark with growing φ_o. Positive error grows with φ_0 while negative error stays bounded above -2º. We note that there is a region where drawing both curves and taking their average by drawing between them would provide a better approximation, but the added effort defeats the purpose. Taken in their proper regions, these approximations hold quite well until $\varphi_0 = 60^\circ$, always keeping the error below 2º, which is probably within the interval for measuring/drawing errors anyway. For larger values of φ_0 the curves take their characteristic sigmoid shape and one should use the general construction of the previous section.

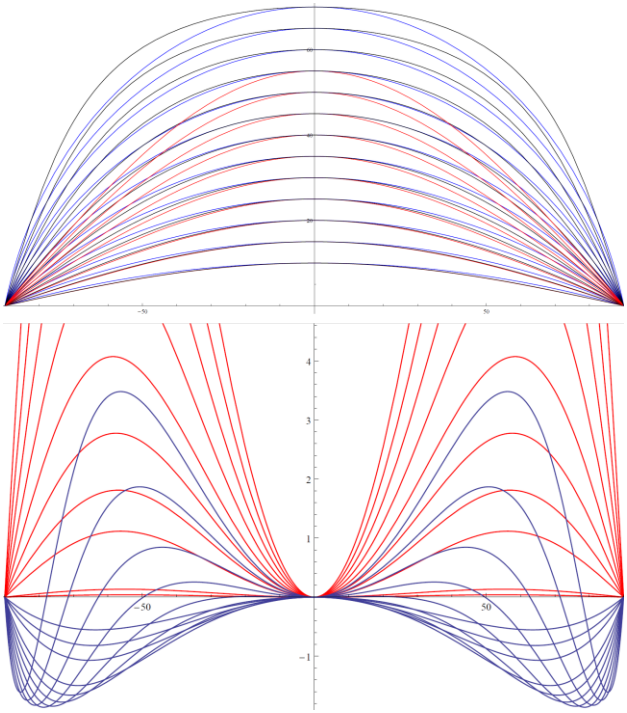

Figure 8 | Top: Plot of horizontals (black) with $\varphi_0 = 10^\circ$ to $\varphi_0 = 70^\circ$ in 5º increments, and of sinusoidal (red) and circular (blue) approximations. Sinusoids omitted for $\varphi_0 > 55^\circ$. Bottom: Plot of the errors of the approximations above. The error of the sinusoids (red) is always positive, with a single maximum near the 60º mark. For circles (blue), it starts negative for small φ_0, with a single minimum, and then develops two extrema with both negative and positive errors. The minimum stays above the -2º mark and maximum grows with φ_0, its latitude shifting nearer to $\pm 90^\circ$.

2.5 UNIFORM GRIDS

The construction of uniform grids is the *pons asinorum* in the study of a perspective. Passing it means the student is ready to begin the real work. Let us consider here only a very simple example of what would be a one-point perspective grid in classical perspective: a tiled box, as in Figure 1. In that picture the box is cubical of side $2d$ and has been tiled with squares of side $d/4$, with a grid crossing under the viewpoint O which is at the center of the box. We solve this grid as follows: Set 0^0 latitude along a grid axis and measure the latitudes of the grid points on the floor along the $\lambda = 0^\circ$ plane. This can be done by direct observation (with a clinometer [1]) or by the diagram of Figure 9 (left) with a protractor. This diagram represents an orthographic side view of the box, with the dots marking the box divisions on the floor and on the facing wall. With the protractor you will obtain four points $P_i = (0, h_i)$ of latitudes $h_i = -90^\circ + \arctan(i/4), i = 1, \ldots, 4$. These are all the measurements you need. Through each of these P_i pass the horizontal $(0, h_i, 0)$. These are the edges of

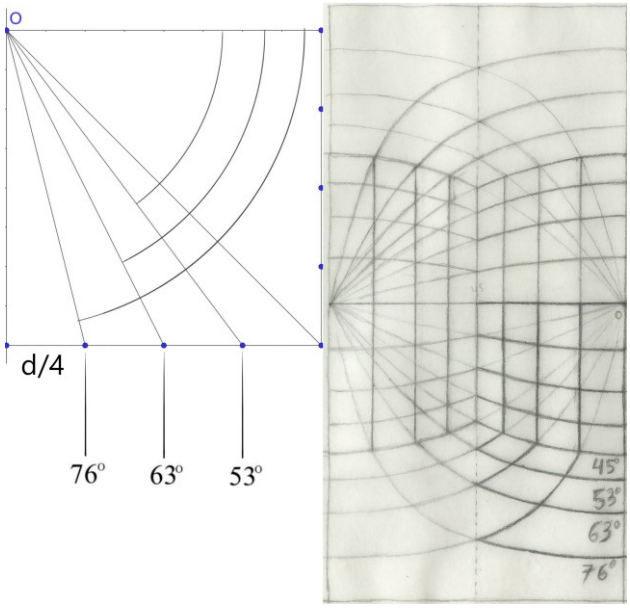

Figure 9 | Left: Protractor measurement of a uniform grid on a box. Right: Equirectangular perspective of a corner of the box. The rest can be obtained by symmetry.

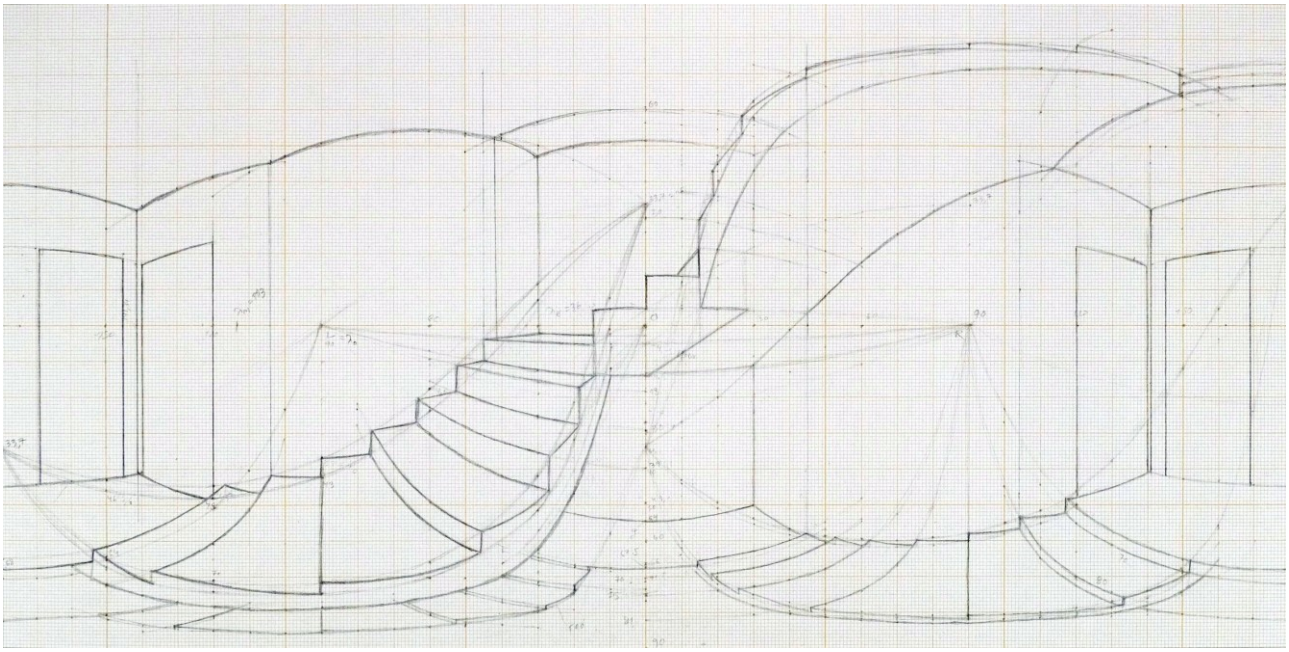

Figure 10 | Equirectangular perspective of a stairwell, with stairs going up and down at 34-degree incline. Notice convergence to vanishing points. Drawing by the author. The VR panorama rendering is available at the author's website (Araújo, 2017c).

the floor tiles that go to your left and right vanishing points (the top one is the edge of the vertical wall, at $\varphi_0 = h_4 = -45^\circ$). To get the orthogonal edges, either repeat the process with your center line facing the left wall ($\lambda = -90^\circ$) or pass a vertical through $\lambda = -45^\circ$ and mirror the lines you have drawn, using the symmetries of the room. You thus obtain the lines of the grid that go to $\lambda = 0$, and in this way a quarter of the tiled floor is achieved (Figure 9, right). To get the horizontal lines of the frontal wall, you might again use the diagram of Figure 9, but notice these angles are mirror images across the 45º line of the angular heights h_i obtained for the floor, so you don't have to measure them; just mirror the points P_i across $\varphi = -45^\circ$. Draw the horizontal lines that go through these at the $\lambda = 0^\circ$ plane and vanish at $\lambda = \pm 90^\circ$, just as you did with the floor horizontals. To get the vertical lines of the wall, pass verticals through the intersections of the floor lines with the bottom edge of the wall. The rest of the box can be tiled by symmetry without further calculation.

Exercise to the reader: extend the floor grid to infinity. You will find the process is analogous to the one used in classical perspective.

Uniform grids of this kind have an interesting property in equirectangular projection: In a sense there is only one of them. If you rotate the room around the z axis, the new drawing will just be displaced by the horizontal offset corresponding to the angle of rotation.

3 | ON THE PRACTICE OF DRAWING

3.1 ON MEASURING

The previous sections assumed access to the variables $\lambda_0, \varphi_0, \theta$. How hard are these to obtain in drawing from life? Direct measurements of φ_0 can be obtained with an improvised clinometer, made from a protractor and a weight on a string, or, less charmingly, with a digital clinometer on a mobile phone. θ can be measured by tilting a pencil in front of one's eyes: by triangle similarity, angles with the horizontal will be preserved as long as the pencil is on a plane parallel to that of the line being measured. Often, circumstances will make some of these variables hard to obtain. Then boxing them inside of horizontals and verticals is useful, among other strategies dictated by circumstance. For example, in Figure 10 there was nothing better for it than just building up a plan and elevation with measuring tape in hand and taking angles from that. Measurement is an art of cunning and circumstance.

3.2 ON GRIDDING

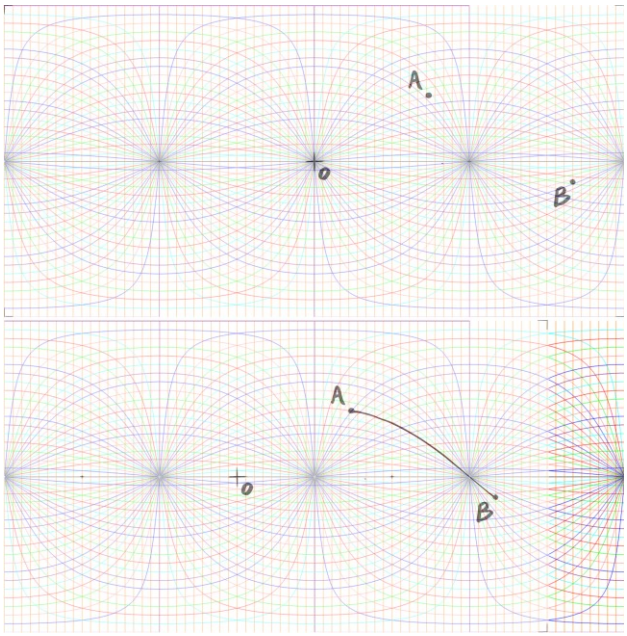

Figure 11 | Top: Two arbitrary points A and B, not in the same horizontal or vertical. Bottom: Horizontal translation of the drafting paper over the grid finds the single great circle that connects A and B – in this case at a 45º shift. This is the value of λ_M, read directly from the new position of mark O. It is much easier to spot the curve when using a grid that is very fine but separates adjacent lines by color, for easy identification when crossing the equator. An adequate grid is available at the author's web site.

The greatest difficulty of this perspective is the awkwardness of the line plots. It is nice to know you can solve them by descriptive geometry, but not something you'd like to do while outdoor sketching. There, you really want to grid. But our study of symmetries has shown that the grid of horizontals and verticals (Figure 4) has more to it than is apparent at first: it is a plot of great circles, and this can be used for a smarter kind of gridding, not limited to drawing horizontals and verticals and guessing the rest. By drawing on tracing paper over such a grid, you can find the single line that joins any two given points A and B. Just slide the grid under your drawing, shifting it horizontally until you find the single great circle that connect them; then trace over it, joining A and B. Our study of symmetries assures us that this works for lines of any incline – and on top of it, finds you the values of (λ_M, φ_M) graphically. Knowing these symmetries and knowing how to measure and plot all vanishing points, a whole avenue of geometrical constructions analogous to those of classical perspective is opened to the draughtsman, as well as a very practical and quick method for on location sketching (Figure 13). This is a longer discussion that we must leave for further notes and materials on the author's web page.

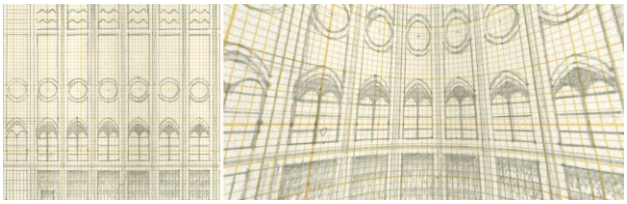

Figure 12 | Left: Author's sketch of the cylindrical reading room and dome of the British Museum viewed from its axis. Rotational symmetry around the z axis reduces the drawing to a simple tile pattern. Right: Snapshot of the VR panorama.

3.3 ON HOW IT MEASURES UP

All said and done, how well does this perspective measure up against the alternatives? Its greatest failing is the awkwardness of line plots for high φ_0, but outdoor sketching can focus on eyeballing shapes and measuring angles, and accurate plotting done later back in the studio; or some smart gridding can be called upon, using the symmetries pointed out above. All in all, I think this perspective compares favorably with cylindrical perspective in the drawing experience. Often the latter suffers from mixing two kinds of measurements (angles and their tangents), and the line plots, as we have seen, are similar for low φ_0 ; just the more limited domain to which cylindrical perspective is by its nature restricted. As for azimuthal equidistant perspective, it remains the most natural spherical perspective, with the simplest line images, but it renders on a disc, which is sometimes objectionable to the artist, and always awkward for conversion to VR. Also, scene symmetries are crucial for the choice (Figure 12), and equirectangular is often better where top and bottom are not the focus (landscapes). There it aligns well with intuition and makes it easier to improvise figures and action on top of carefully planned referential backdrops.

4 | CONCLUSION

Equirectangular perspective is an attractive option for drawing panoramas. It is a full spherical perspective, yet carries the symmetries of cylindrical perspective in good approximation for low latitudes. VR visualization makes it useful both for the student of geometry, who can validate constructions in anamorphosis and for the artist interested in the interface between analog and digital drawing. Its main defect is the complexity of high-latitude line projections, but these can be solved by achieving a few points through descriptive geometry, the rest following by symmetry. We have given a brief outline of a procedure for plotting these lines with elementary tools: ruler, compass, and protractor.

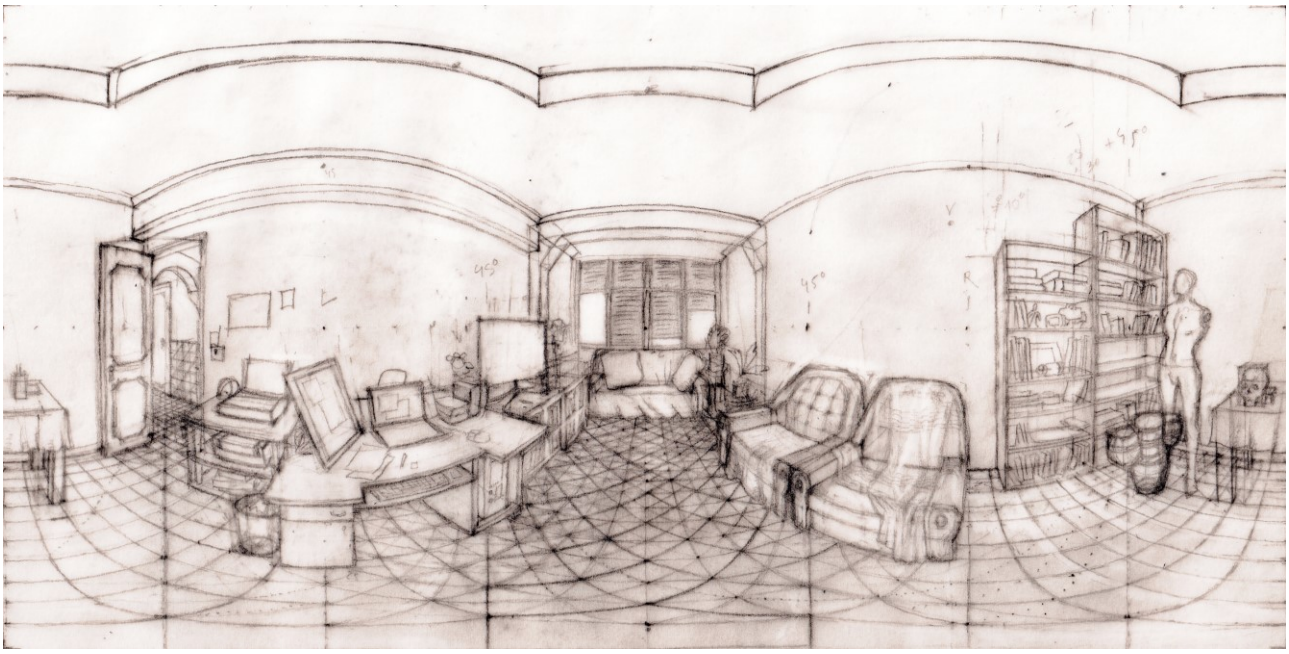

Figure 13 | Sketch of a room from observation, using the tracing technique of section 3.2 and enlarging the uniform grid construction of section 2.5 through the use of 45º diagonals. See VR panorama at author's website.

There is an art, however, to knowing what to measure and where to start. Solving a perspective mean also giving a corpus of solved problems that help the artist in framing the most common situations, and in this we have here by necessity been terse to a fault. The reader will find in due course further notes, illustrations and VR panoramas at the author's website (Araújo, 2017c).

ACKOWLEDGMENTS

This work was supported by Artech-Int, Associação Internacional de Arte Computacional, and by Portuguese national funds through FCT- Fundação para a Ciência e a Tecnologia, within project UID/Multi/04019/2013.

ENDNOTES

[1] A clinometer is a device for measuring the angular elevation of a target. It may be improvised thus: nail a tube to a protractor so that they move together, and hang a weight from the nail by a thread, to mark the vertical. When you spot the target through the tube, the vertical thread will mark the angular elevation on the protractor.

REFERENCES

Anderson, D. (n.d.). panorama illustrations. Retrieved April 19, 2017, from https://www.flickr.com/photos/davidanderson/sets/72157627385462893

Araújo, A. (2015). A Construction of the Total Spherical Perspective in Ruler, Compass and Nail. Retrieved from http://arxiv.org/abs/1511.02969

Araújo, A. (2017). Guidelines for drawing immersive panoramas in equirectangular perspective. In C. Caires (Ed.), Artech 2017. International Conference on Digital Arts, 8 - "Interfaces of Tomorrow". Macau: ACM.

Araújo, A. (2017a). Anamorphosis: Optical Games with Perspective's Playful Parent. In J. N. Silva (Ed.), Recreational Mathematics Colloquium V G4G (pp. 71-86). Lisbon: Ludus.

Araújo, A. (2017b). Cardboarding Mixed Reality with Dürer Machines. 5th Conference on Computation, Communication, Aesthetics & X (pp. 102-113). Lisbon: Univ. do Porto. Retrieved from http://2017.xcoax.org/xCoAx2017.pdf

Araújo, A. (2017c). Notes and materials on equirectangular perspective and VR panoramas. Retrieved from http://www.univ-ab.pt/~aaraujo/equirectangular.html

Art Panorama Group. (2017, April 19). Art Panoramas. Retrieved from Flickr: https://www.flickr.com/groups/artpanoramas/pool/

Barre, A., & Flocon, A. (1964). La perspective Curviligne. Paris: Flammarion.

Barre, A., Flocon, A., & Bouligand, G. (1964). Étude comparée de différentes méthodes de perspective, une perspective curviligne. Bulletin de la Classe des Sciences de La Académie Royale de Belgique, Série 5, Tome L.

Huhtamo, E. (2013). Illusions in motion - media archaeology of the moving panorama and related spectacles (1st ed.). London: The MIT Press.

Kemp, M. (1990). The Science of Art. New Haven and London: Yale University Press.

Michel, G. (2007). L'oeil, au Centre de la Sphere Visuelle. Boletim da Aproged, 3-14.

Michel, G. (2017, April 19). Dessin à main levéee du Cinéma Sauveniére. Retrieved from http://autrepointdevue.com/blog/wp-content/vv/vv-gm-sauveniere/vv-gm-sauveniere.html

Papert, S., & Turkle, S. (1991). Epistemological Pluralism. In I. a. Harel (Ed.), Constructionism (pp. 161-191). Ablex Publishing Co.

Pozzo, A. (1700). Perspectiva pictorum et architectorum, vol 2. Rome.

Rodriguez, H. (2016). Theorem 8.1. 4th Conference on Computation, Communication, Aesthetics and X, (pp. 333-340). Bergamo.

Snyder, J. (1987). Map Projections - a Working Manual (Vol. 1935). Washington, U.S.A.: U.S.G.P.O.

Stiegler, B. (2010). For a New Critique of Political Economy. Cambridge: Polity Press.

Termes, D. (n.a.). New Perspective Systems. self-published.

BIOGRAPHICAL INFORMATION

António Bandeira Araújo is a geometer and draughtsman. He holds a degree in physics and a Ph.D. in mathematics. He had training in drawing, painting, and scientific illustration, and has published illustration work. His main interest lies in the interactions between mathematics and the visual arts, both classical and digital. He lectures at Universidade Aberta in Portugal and is a member of CIAC-UAb (Centro de Investigação em Artes e Comunicação) and CMAF-CIO (Centro de Matemática, Aplicações Fundamentais e Investigação Operacional).